

Effect of biaxial strain and composition on vacancy mediated diffusion in random binary alloys:

A first principles study of the $\text{Si}_{1-x}\text{Ge}_x$ system

Panchapakesan Ramanarayanan* and Kyeongjae Cho

Department of Mechanical Engineering, Stanford University, Stanford, California 94305

Bruce M. Clemens

Department of Materials Science and Engineering, Stanford University, Stanford, California 94305

We present the results of a systematic study using the density functional theory (within the local density approximation) of the effects of biaxial strain and composition on the self-diffusion of Si and Ge in $\text{Si}_{1-x}\text{Ge}_x$ alloys diffusing by a vacancy mechanism. The biaxial strain dependence of the vacancy formation energy was reconfirmed with previous calculations. The effect of biaxial strain on the interaction potential energy between a substitutional Ge atom and a vacancy was calculated. The interaction potential energy included not only the ground state energies of the vacancy at different coordination sites from the Ge atom but also the migration energy barriers to jump from one coordination site to the adjacent. These calculations were used to estimate the change in the activation energy (due to biaxial strain) for the self-diffusion of Si and Ge in Si by a vacancy mechanism. The composition dependence of the vacancy formation energy was calculated. A database of *ab initio* migration energy barriers for vacancy migration in different local environments was systematically developed by considering the effect of the first nearest neighbor sites explicitly and the effect of the other sites by a mean field approximation. A kinetic Monte Carlo simulation based on the migration energy barrier database was performed to determine the dependence (on the composition) of the activation energy for the diffusion of Si and Ge in $\text{Si}_{1-x}\text{Ge}_x$. A detailed study of the variation of the correlation factor with composition and temperature in $\text{Si}_{1-x}\text{Ge}_x$ was performed using the results of the KMC simulation. These analyses constitute essential building blocks to understand the mechanism of vacancy mediated diffusion processes at the microscopic level.

I. INTRODUCTION

Silicon germanium technology is becoming increasingly popular in high frequency, low power applications,¹ the principal reasons being the advancement in precision growth technologies² and the compatibility of $\text{Si}_{1-x}\text{Ge}_x$ with the Si manufacturing processes along with such properties of $\text{Si}_{1-x}\text{Ge}_x$ as the composition dependence of the band gap, the strain dependence of the carrier mobility, and the increased dopant solubility in $\text{Si}_{1-x}\text{Ge}_x$ compared to Si. The abrupt change in the Ge concentration between the Si and the $\text{Si}_{1-x}\text{Ge}_x$ layers being a functional necessity in these devices, a key materials issue is that of interdiffusion in these layers. There have been extensive studies of this stress-coupled interdiffusion.^{3,4,5,6,7,8,9,10} Yet, a lot about the actual microscopic mechanisms behind these phenomena remains to be understood. Similarly the microscopic mechanisms responsible for the growth, composition, and the shape of $\text{Si}_{1-x}\text{Ge}_x$ islands on Si, which find applications in areas like Si-based quantum dots, are also not well understood. From a technological standpoint, understanding diffusion in $\text{Si}_{1-x}\text{Ge}_x$ is therefore important. From a scientific standpoint, the silicon germanium system presents an ideal and clean system (without the complications introduced by charged defect states) to further the theoretical understanding of interdiffusion in random alloys in general. Quoting from a recent paper,¹¹ “Theoretical treatments of self-diffusion in SiGe are uncharted areas - and the effect of strain even

more so.” These reasons have motivated us to perform a systematic and detailed first principles study of the $\text{Si}_{1-x}\text{Ge}_x$ system.

In their recent paper, Zangenberg *et al.*¹¹ have presented their results of a systematic experimental study of the variation of Ge self-diffusion in mono crystalline $\text{Si}_{1-x}\text{Ge}_x$ epi-layers as a function of composition (x) and biaxial strain. (A similar study has also been reported by Strohm *et al.*¹²) These works represent an advancement over that presented by McVay and DuCharme¹³ in 1974, which studied the composition dependent Ge diffusion in polycrystalline $\text{Si}_{1-x}\text{Ge}_x$. These results have been used in the past as an input to empirically explain other experimentally observed phenomena. For example, Baribeau⁴ used the Ge dependent diffusivity from Ref. 13 to numerically solve the one dimensional Fick’s diffusion equation and compared the results with those of the experimentally determined ones. Similarly, Aubertine *et al.*³ have used the Ge dependent diffusivity from Ref. 11 in a commercial numerical solver to perform a similar comparison with their experiments to provide an empirical explanation to the experimentally observed time dependent interdiffusivity in Si/ $\text{Si}_{1-x}\text{Ge}_x$ multilayers. Thus, although these results (of Refs. 11,12,13) have been valuable in providing empirical insights into other phenomena, the reasons for these behaviors themselves have not been queried into from a fundamental level, to the best of our knowledge. We are aware, however, of a recent paper by Venezuela *et al.*¹⁴ that has made an attempt in

this direction.

Our present work is a part of a project intended to develop a fundamental understanding at the microscopic level ultimately, of the coupled strain relaxation and interdiffusion phenomenon in Si/Si_{1-x}Ge_x multilayers. Towards this end, a fundamental understanding of the strain and composition dependent diffusivity in Si_{1-x}Ge_x as observed by the experiments mentioned previously^{11,12,13} is an essential prerequisite. Diffusion in SiGe has been postulated¹⁵ to be mediated by point defects: vacancies, interstitials and by a point defect free mechanism - the concerted exchange mechanism. Very recently, another point defect, which the authors¹⁶ have termed the fourfold coordinated defect (FFCD), has been suggested which could also be responsible for diffusion in SiGe. From their experimental observations, Fahey *et al.*¹⁷ suggest that at 1050 °C, the vacancy mechanism probably contributes to 60% - 70% of the Ge diffusion in Si, the rest being due to the interstitial mechanism. We note that the results presented in Ref. 17 are for the diffusion of Ge in pure Si and so the relative contributions of the different mechanisms could be different for systems with different Ge concentrations. However, because vacancies are among the important contributors, they are the focus of this article.

Density functional theory (DFT) calculations have played a significant role in computational physics during the past few decades since the theory's formal inception in the mid 1960s. The unknown nature of the exchange correlation functional and the inability to make progressively more accurate approximations to the same (as would be possible, for example, in a wave function based method), however, has been one of the main issues concerning the practical application of the DFT. The search for better exchange correlation functionals is an active area of research in the theoretical physics community. The popular local density approximation (LDA) and the more computationally expensive (but not necessarily more accurate) generalized gradient approximation (GGA), unfortunately, have been unable to reproduce experimentally observed values of activation energy of diffusion in Si, the discrepancy¹⁸ being as high as 1eV. Quantum Monte Carlo techniques,^{19,20} which circumvent the problem due to the exchange correlation functional, are gaining popularity. However, because the LDA based DFT is definitely one of the most advanced computational tools available for the systems of the size that we would like to study, we have used it in this present study. Because we are aware of this discrepancy between the theoretical prediction and the experimental values, and because we have restricted this present article to only the vacancy mechanism, we prefer to refrain from making very strong comparisons of our results with those of experiments, leaving such comparisons to the future until we have resolved these outstanding issues. In spite of these limitations, we believe that our contribution is significant for the following two reasons: (i) Our results can be viewed as that of the behavior of a hypotheti-

cal random binary alloy system (with the energetics provided by the LDA) diffusing by a vacancy mechanism. This is of basic scientific interest. (ii) The infrastructure that we have developed in this present work can be reused with little effort once accurate energetics becomes available. This, along with similar analyses for other diffusion mechanisms can then be used to directly compare/predict experimental observations.

Because diffusion is a thermally activated process, diffusivity can be characterized by a temperature independent term (the pre-exponential factor, D_0) and a temperature dependent term (the exponential of the activation energy, E_a , i.e., $\exp[-E_a/k_B T]$ where k_B and T are respectively the Boltzmann's constant and the temperature). For a defect mediated diffusion mechanism, the activation energy (E_a) is composed of the defect formation energy and the rest, which we have termed as the activation-minus-formation (AMF) energy. We note that this has traditionally been called as the migration energy. The reason we have not called it the migration energy needs some explanation. We first consider the case of a tracer self diffusion. Shown in Fig. 1, for the sake of illustration, is the motion of a tracer in a two dimensional hexagonal lattice from an initial state to the final through the saddle point. The migration energy in this case has a very direct physical significance, namely, the energy difference between the saddle point and the initial (ground) state. But when one considers anything other than a unary system, for example the diffusion of a tracer Ge in Si, one is unable to make a physically appealing correspondence to a migration process as in the case of a tracer self diffusion in a unary system. Specifically, considering the illustration shown in Fig. 2, for the Ge atom (filled circle) to be effectively displaced from its current position (labelled 1), the vacancy (filled square) has to move from its current position (labelled 2) to atleast the third coordination site from Ge (labelled 8) and return by another path (for example through sites labelled 6 and 3). As shown in Fig. 3, there are different energy barriers to get to different configurations: the barrier for the vacancy to get from the first coordination site (from Ge) to the second is different from that to get from the second to the third. The contribution to the activation energy (other than the effective defect formation energy) is not only from the complex collective action of all these different migration barriers but also, in this particular pair diffusion model, due to the energy required for the vacancy to get to the third coordination site, for example, so that it can return to the Ge atom from a different direction thereby causing a net motion of the Ge atom. These complex collective actions manifest in different forms, for example, as a temperature dependent correlation factor. Therefore, we felt the need to make the distinction from the term: migration energy. The AMF energy equals the migration energy in the microscopic sense only for the case of the tracer self-diffusion in a unary system. Although previous reports^{21,22,23} have suggested different measures of an effective migration barrier for these

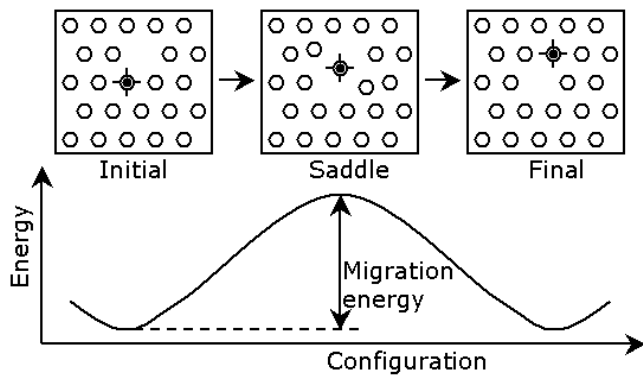


FIG. 1: Migration energy for the motion of a tracer (shown as the target symbol) in a unary system has a direct physical correspondence: difference between the saddle point and the ground state energies.

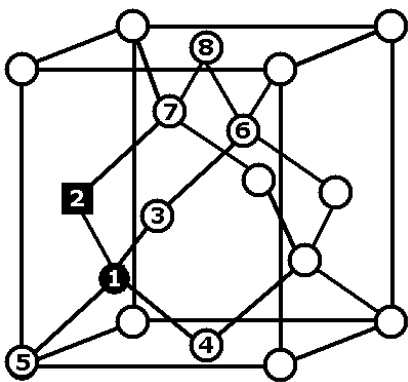


FIG. 2: Schematic of the Si structure. Open circles - Si; filled circle - Ge; filled square - vacancy.

cases, we remark that we do not find any of them physically enlightening.

In order to study the effect of biaxial strain and composition on the diffusivity, one needs to study their effect on these three parameters, viz., the pre-exponential factor (D_0), the vacancy formation energy, and the AMF energy. Several previous first principles calculations^{23,24,25,26} have reported on the strain dependence of vacancy formation energy. In this article, we present our results where we have reconfirmed the biaxial-strain dependence of the vacancy formation energy. Though we have seen general theoretical treatments^{27,28} of the effect of strain on defect diffusion, we have not come across any reference reporting on the *ab initio* based calculation of the variation of the AMF energy (or the effective migration energy as it is generally known) as a function of strain. In this article, we have calculated the biaxial strain dependence of the interaction potential energy between a substitutional Ge atom and a vacancy. The interaction potential energy included not only the ground state energies of the vacancy at different coordination sites from the Ge atom but also the migration energy barriers for jumps from

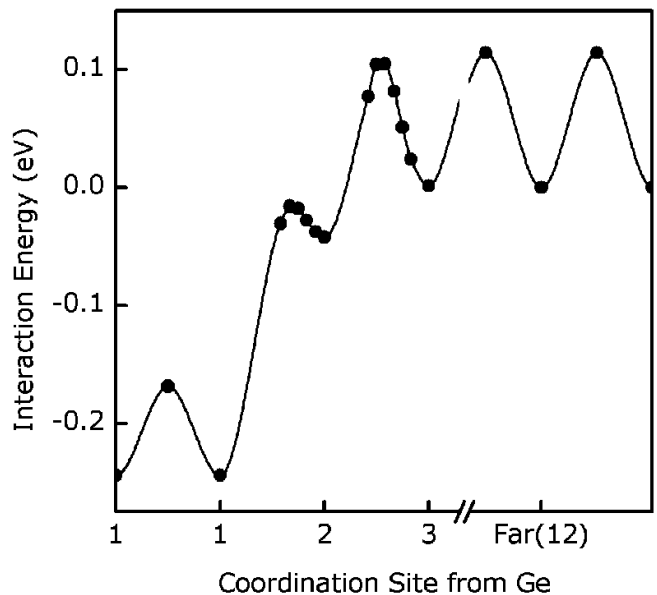


FIG. 3: Interaction potential energy (in eV) between a substitutional Ge atom and a vacancy as a function of vacancy position in relaxed Si from LDA calculations. (Lines are drawn as a guide to the eye.)

one coordination site to the adjacent. We have used these calculations to estimate the change in the activation energy (due to biaxial strain) for the self-diffusion of Si and Ge in Si by a vacancy mechanism. We then present our calculations of the Ge concentration dependence of the vacancy formation energy where we have used the classic Boltzmann factor enhancement of the probabilities. We note that Venezuela *et al.*¹⁴ have used an approach similar to ours in their recent paper. Earlier theoretical or numerical studies^{21,29,30,31} have only reported on the analyses of the concentration dependence of diffusivity in the low concentration regime, typically those corresponding to dopant concentrations. We have not found theoretical or numerical treatments of the concentration effects on diffusivity for higher solute concentrations like those found in $\text{Si}_{1-x}\text{Ge}_x$ alloy systems. We present the variation of the AMF energy as a function of Ge concentration, which we have obtained from kinetic Monte Carlo (KMC) simulations using a migration energy barrier database calculated from first principles. The KMC simulations also enabled us to study the variation of the correlation factor as a function of Ge concentration and temperature. Such a study provides useful insight into the vacancy mediated diffusion mechanism in a random binary alloy arranged in a tetrahedral geometry.

This article is organized as follows: In section II, we present the theoretical details of our calculations and the computational details of our simulations. In section III, we discuss our main results. In section IV, we conclude the article with a summary of the present work and also comment on the limitations of this work.

II. THEORETICAL AND COMPUTATIONAL DETAILS

In this section, we present the theory behind our calculations and the main computational details of our simulations.

A. First principles calculations

Our first principles calculations were performed using the plane-wave ultrasoft pseudopotential code VASP^{32,33,34,35} within the local density approximation (LDA). A 64-atom supercell with a kinetic energy cut-off of 10 Hartree, and a 2^3 Monkhorst-Pack³⁶ \mathbf{k} -point sampling was used. Electronic energy convergence of up to 2.7×10^{-5} eV was used and the structures were relaxed until the maximum force on any atom was less than 0.015 eV/Å. Saddle point configurations were determined using the nudged elastic band (NEB) method.³⁷ Optimized Si and Ge lattice constants (computed by fitting the total energy vs. the supercell volume to Murnaghan's^{38,39} equation of state) were found to be 5.39 Å and 5.62 Å respectively. The vacancy formation energy and the vacancy formation volume in Si (Ge) were found to be 3.31 (1.88) eV, and -0.059 (-0.195) Ω respectively where Ω represents the volume of a Si (Ge) atom. (We recall that the vacancy formation volume is the sum of the relaxation volume (Si: -20.73 \AA^3 ; Ge: -26.56 \AA^3) and the atomic volume (Si: 19.57 \AA^3 ; Ge: 22.23 \AA^3 .) These values are expectedly comparable to other recent first principle calculations.^{40,41,42,43} Because of the low Si-vacancy formation volume and because of $\text{Si}_{1-x}\text{Ge}_x$ being a model random alloy,^{44,45} the lattice parameters for $\text{Si}_{1-x}\text{Ge}_x$ were chosen by a simple rule of mixtures. Lattice parameters so chosen were assumed to correspond to a strain relaxed state. Unless otherwise mentioned, all our calculations were done in such a strain relaxed state.

B. Kinetic Monte Carlo simulations

The diamond lattice was generated in the computer memory by a four-dimensional integer array. The first three indices were used to reference the location (i.e., X,Y,Z “coordinates”) of the cubic unit cell. The last index was used to reference the particular atom among the eight in the unit cell referred to by the first three indices. Because $\text{Si}_{1-x}\text{Ge}_x$ forms a random alloy,^{44,45} each member of this array was randomly designated as either a Si atom or a Ge atom and one randomly chosen member was designated as the vacancy. The relative numbers of the Si and Ge atoms were so chosen that the required composition was obtained. The displacement and the number of jumps performed by each of these atoms were recorded through out the simulation. Periodic boundary conditions were used so that an atom hopping out

of one side reenters the system from the opposite side, essentially simulating an infinite system.

Each KMC move consisted of the following five steps: (i) Obtaining the rates r_i for the possible final configurations starting from the current configuration as the initial configuration. (ii) Generating a pseudo-random number $\gamma \in (0, 1]$. (iii) Advancing the clock⁴⁶ by $-\ln(\gamma)/\sum_i r_i$. (iv) Reconfiguring the system into one of the final configurations based on the random number generated in step (ii). (v) Updating the displacement and the number of jumps of the vacancy and the atoms that have moved. We refer the reader to the original KMC paper by Voter⁴⁷ for details on the theory of the kinetic Monte Carlo algorithm.

The supercell comprised of $50 \times 50 \times 50$ cubic unit cells each containing eight lattice sites making up one million lattice sites. Random alloys of $\text{Si}_{1-x}\text{Ge}_x$ with the concentration of Ge (x) varying from 0 to 1 were used to study the effect of composition. A single vacancy was used. (We note that the presence of one vacancy in a $50 \times 50 \times 50$ super cell, which we are forced to use due to computational limitations, results in an extremely high concentration of vacancy compared to the real $\text{Si}_{1-x}\text{Ge}_x$ system.) Three different random distributions of Ge atoms were used for each composition and three different random number sequences were used for each distribution, thus making up nine samples for each composition. The results were averaged over all the nine samples. A billion vacancy hops were performed for each case. The scatter in the results among these nine samples was found to be extremely low.

C. Effective vacancy formation energy calculation

In this subsection, we explain how we use the classic Boltzmann factor to calculate the effective vacancy formation energy in the $\text{Si}_{1-x}\text{Ge}_x$ alloy (where x denotes the atomic fraction of Ge). The strength of the interaction between a vacancy and a Ge atom is expectedly dependent on their relative positions. The interaction of the vacancy with the Ge atoms which are first nearest neighbors to the vacancy is stronger than with those which are second nearest neighbors. This second nearest neighbor interaction in turn is stronger than between those which are further away. We have therefore chosen three different forms to represent these three different interactions. For the strongest interaction, we define a function F . We denote as $F(b)$ the drop in energy of the system when a vacancy is surrounded by b Ge atoms at the first nearest neighbor position to the vacancy. (For the Si structure, b , of course, ranges from zero through four.) For the interaction between the vacancy and Ge atoms that are at the second nearest neighbor positions to the vacancy, we use a linear expression for the drop in the energy with the number of Ge atoms in the second nearest neighbor position. We denote the constant of proportionality i.e., the drop in energy of the system for each Ge atom

in the second nearest neighbor position as S . Because the interaction between the vacancy and Ge atoms that are present beyond the second nearest neighbor positions is comparatively weak, we consider their effect through a mean field correction factor: M . M is the difference between the energy of a system with a vacancy whose first and second nearest neighboring positions are occupied by Ge atoms and all other positions are occupied by Si atoms and that of a system with a vacancy with Ge atoms in all the positions. We denote as $E(n, b, x)$ the vacancy formation energy in a $\text{Si}_{1-x}\text{Ge}_x$ system (with a Ge concentration of x). Here, n denotes the total number of Ge atoms in the first and second nearest neighbor positions to the vacancy and b denotes the number of Ge atoms that are in the first nearest neighbor positions to the vacancy. We then obtain the following expression for $E(n, b, x)$ in terms of the vacancy formation energy in pure Si ($E_{V_f}^{\text{Si}}$) and the quantities F , S , and M defined above:

$$E(n, b, x) = E_{V_f}^{\text{Si}} - F(b) - (n - b)S - Mx \quad (1)$$

If the distribution of Ge atoms is unaffected by vacancies, then, the probability $\tilde{p}(n, b, x)$ of a vacancy being surrounded by n Ge atoms, b of which are first nearest neighbors to the vacancy and the rest $(n - b)$ are second nearest neighbors is calculated in the following manner using the binomial Bernoulli distribution from elementary probability theory: (Note: There are 4 first nearest

neighbor sites and 12 second nearest neighbor sites in the diamond lattice.) The probability of a vacancy being surrounded by b Ge atoms in the first nearest neighbor position is $\binom{4}{b}x^b(1-x)^{4-b}$ (where x is the concentration of Ge). The probability of a vacancy being surrounded by $(n - b)$ Ge atoms in the second nearest neighbor position is $\binom{12}{n-b}x^{n-b}(1-x)^{12-(n-b)}$. The required probability $\tilde{p}(n, b, x)$ is therefore the product of the above two which simplifies to the following expression:

$$\tilde{p}(n, b, x) = \binom{4}{b} \binom{12}{n-b} x^n (1-x)^{16-n} \quad (2)$$

The interaction between the Ge and the vacancies, however, affects their distribution. The probability $p(n, b, x, T)$, which takes this interaction into account, is obtained by multiplying $\tilde{p}(n, b, x)$ by the Boltzmann factor corresponding to the energy drop because of this interaction. We thus obtain the following expression for $p(n, b, x, T)$:

$$p(n, b, x, T) = \tilde{p}(n, b, x) \exp[(F(b) + (n - b)S)/k_B T] \quad (3)$$

where k_B is the Boltzmann's constant and T is the temperature. We then express the effective vacancy formation energy, $\langle E_f(x, T) \rangle$, as an average of the vacancy formation energies in the different environments weighted by their corresponding probabilities:

$$\langle E_f(x, T) \rangle = \frac{1}{z} \left[\sum_{n=0}^4 \left(\sum_{b=0}^n p(n, b, x, T) \times E(n, b, x) \right) + \sum_{n=5}^{16} \left(\sum_{b=0}^4 p(n, b, x, T) \times E(n, b, x) \right) \right] \quad (4)$$

where z is like the partition function:

$$z = \sum_{n=0}^4 \left(\sum_{b=0}^n p(n, b, x, T) \right) + \sum_{n=5}^{16} \left(\sum_{b=0}^4 p(n, b, x, T) \right) \quad (5)$$

We make the following two clarifications: (i) We have not included the mean field correction term M in the expression for the Boltzmann factor in Eq. (3) because, M being independent of n or b , is factored out of the numerator and the denominator (z) in the expression for $\langle E_f(x, T) \rangle$ (Eq. (4)) even if it is included. (ii) We have two terms in the RHS of Eqs. (4) and (5) for the following simple reason: The number of first nearest neighbor Ge atoms (b) can be at most equal to the total number of Ge atoms in the first and the second nearest neighbor positions (n) when n is less than or equal to four. This is the first term on the RHS. The variable b can be at most equal to four when n is greater than four. This is the second term.

D. Theoretical calculation of correlation factor

The correlation factor (f) is defined⁴⁸ as the ratio of the actual diffusion coefficient to the uncorrelated diffusion coefficient under the assumption that all the jumps are statistically independent of one another. The correlation factor provides a lot of insight into the microscopic mechanism of diffusion. In this sub-section, we give a brief outline of how the correlation factor is computed. We refer the reader to Ref. 48 for further details. The correlation factor for the diffusion of a single impurity atom in a cubic crystal by the vacancy mechanism can be calculated using the expression:

$$f = \frac{1 + \langle \cos \theta \rangle}{1 - \langle \cos \theta \rangle} \quad (6)$$

Here, $\langle \cos \theta \rangle$, which denotes the average of the cosine of the angle between successive impurity jumps, can be evaluated as $T_j \cos \theta_j$. T_j is the probability for the impurity to jump to the j^{th} configuration. θ_j is the angle formed

between the current impurity jump direction and the impurity jump direction leading to the j^{th} configuration. There is the implicit sum over the repeated index j . In the case of the diamond structure, j ranges over the four first nearest neighbors; i.e., the j^{th} configuration results when the impurity jumps to the j^{th} first nearest neighbor. Referring to Fig. 2, where the destination configurations (i.e., first nearest neighbors to impurity) are denoted by the numbers 2 through 5, the probabilities T_2 through T_5 have been calculated by including jump sequences up to five vacancy hops⁴⁹ in the following manner: We denote respectively by ν_I , ν_H , ν_F , and ν_B , the jump rates for the following vacancy jump processes: (i) Vacancy exchanges positions with the impurity atom. (ii) Vacancy exchanges positions with the host atom without either breaking or forming a bond with the impurity atom. (iii) Vacancy exchanges positions with the host atom and in the process *forms* a bond with the impurity atom. (iv) Vacancy exchanges positions with the host atom and in the process *breaks* a bond with the impurity atom. (We explain the procedure for obtaining the values of the various jump rates (ν_I , ν_H , ν_F , and ν_B) from our LDA calculations in Sec. III A.) We denote as $R(j, k)$ the probability for the impurity to jump to the j^{th} first nearest neighbor position as a result of the vacancy performing k hops. (For example (referring to Fig. 2), one of the ways in which the impurity atom can jump to the first nearest neighbor position denoted as 2 as a result of the vacancy performing three hops would be the following jump sequence of the vacancy: 2 to 7 followed by 7 to 2 followed by 2 to 1.) Using elementary probability theory, the various $R(j, k)$'s can be computed to obtain:

$$R(2, 1) = \frac{\nu_I}{\nu_I + 3\nu_B} \quad (7)$$

$$R(2, 3) = 3 \times \frac{\nu_B}{\nu_I + 3\nu_B} \times \frac{\nu_F}{\nu_F + 3\nu_H} \times \frac{\nu_I}{\nu_I + 3\nu_B} \quad (8)$$

$$R(2, 5) = 9 \times \frac{\nu_B}{\nu_I + 3\nu_B} \times \frac{\nu_H}{\nu_F + 3\nu_H} \times \frac{1}{4} \times \frac{\nu_F}{\nu_F + 3\nu_H} \times \frac{\nu_I}{\nu_I + 3\nu_B} \quad (9)$$

$$R(3, 5) = R(4, 5) = R(5, 5) = 2 \times \frac{\nu_B}{\nu_I + 3\nu_B} \times \frac{\nu_H}{\nu_F + 3\nu_H} \times \frac{1}{4} \times \frac{\nu_F}{\nu_F + 3\nu_H} \times \frac{\nu_I}{\nu_I + 3\nu_B} \quad (10)$$

The $R(j, k)$'s not listed above are all zero. T_j is then obtained by simply summing $R(j, k)$ over k from one through five.⁴⁹ We obtain the following expressions, in terms of the various $R(j, k)$'s, for the probabilities T_2 through T_5 :

$$T_2 = R(2, 1) + R(2, 3) + R(2, 5) \quad (11)$$

$$T_3 = T_4 = T_5 = R(3, 5) \quad (12)$$

Also, from Fig. 2, $\cos\theta_2 = -1$ and $\cos\theta_3 = \cos\theta_4 = \cos\theta_5 = 1/3$.

E. Calculation of the correlation factor from the KMC simulation results

The procedure for calculating the correlation factor outlined in Sec. IID is valid only for a single impurity atom migrating by a vacancy mechanism. Certain symmetry requirements, which were implicitly used in the formulae presented there, are violated at higher impurity concentrations. In this subsection, we explain the procedure for calculating the correlation factor that is valid for any impurity composition, as long as there are a sufficient number of atoms to obtain a good statistical average. This procedure is a straightforward interpretation of the definition of the correlation factor as applied to the results from the KMC simulation.

From the definition of the correlation factor as the ratio of the actual diffusivity to the uncorrelated diffusivity and from the definition of the diffusivity as the ratio of the mean squared displacement $\langle X^2 \rangle$ to 6τ , where τ is the time taken for the motion in the limit as τ tends to zero, we obtain the correlation factor to be the ratio of the actual mean squared displacement to the mean squared displacement when the motion is uncorrelated. Symbolically,

$$f = \frac{\langle X^2 \rangle_{\text{actual}}}{\langle X^2 \rangle_{\text{random}}} \quad (13)$$

From the random walk analysis, $\langle X^2 \rangle_{\text{random}} = \langle N \rangle \lambda^2$, where $\langle N \rangle$ is the mean number of jumps and λ is the single jump distance. For the diamond structure, $\lambda = 0.25\sqrt{3}$ (in units of the unit cell dimension) and so we obtain the correlation factor to be

$$f = \frac{\langle X_x^2 \rangle + \langle X_y^2 \rangle + \langle X_z^2 \rangle}{3 \times (0.25)^2 \times \langle N \rangle} \quad (14)$$

From the output of the KMC simulation, which has the displacements and the number of jumps of each atom, the mean squared displacements ($\langle X_x^2 \rangle$, $\langle X_y^2 \rangle$, $\langle X_z^2 \rangle$) and the mean number of jumps ($\langle N \rangle$) can be calculated by averaging the quantities over all atoms of the same type (Si or Ge). The correlation factor can thus be calculated in a straightforward manner from the KMC simulation results.

III. RESULTS AND DISCUSSION

A. Biaxial strain dependence of the activation energy

The change in vacancy formation energy due to biaxial strain is computed as⁵⁰ $(-2/3)V_r\mu$ where V_r is the relaxation volume and μ is the biaxial modulus of Si. From our LDA calculations, the relaxation volume accompanying the formation of a vacancy in Si is -20.73 \AA^3 . (The relaxation volume in this case is approximately -1.06 times the atomic volume of Si.) The biaxial modulus⁵¹ of Si is

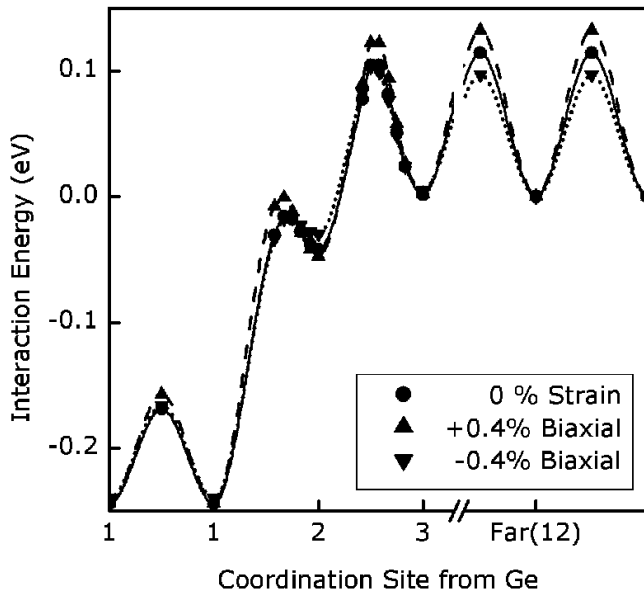


FIG. 4: Interaction potential energy (in eV) between a substitutional Ge atom and a vacancy as a function of vacancy position in (a) relaxed Si (circles connected with solid line) (b) 0.4% tensile biaxially strained Si (upward triangles connected with dashed line) (c) 0.4% compressively biaxially strained Si (downward triangles connected with dotted line) from LDA calculations. The energies of all the systems when the vacancy and the Ge are far apart have been normalized to zero. (Lines are drawn as a guide to the eye.)

190.48 GPa. We therefore find the change in vacancy formation energy due to equi-biaxial strain to be 16 eV/unit strain.

The interaction potential energies of a vacancy with a substitutional Ge atom for (a) relaxed, (b) 0.4% tensile equi-biaxially strained, and (c) 0.4% compressively equi-biaxially strained systems are as shown in Fig. 4. (The interaction potential energy for the relaxed system shown in Fig. 4 is exactly same as that shown in Fig. 3. It has been shown separately in Fig. 3 for the sake of clarity and has been shown in Fig. 4 for the sake of making comparisons with the strained systems.) We make the following comments and observations with reference to Figs. 3 and 4: (i) Our first principles calculations indicate that a biaxial tension (compression) of 0.4% causes the third dimension to contract (expand) by 0.39% (0.46%) in reasonable agreement with that predicted by linear elasticity theory⁵² which gives a contraction (expansion) of 0.31% (0.31%). To maintain consistency, the interaction potential energy calculations were made using the dimensions obtained from our LDA computations. (ii) From Fig. 3 we see that the migration barrier for the vacancy to exchange positions with a Si atom far away from a Ge atom is 0.11 eV. This is as expected, owing to the similarity of the calculation technique, in reasonable agreement with Nelson *et al.*⁵³ who report a value of 0.18 eV from their LDA calculations. (iii) The asymmetric location of the saddle points between the 1st and the 2nd coordination

sites, and the 2nd and the 3rd coordination sites is due to the weaker nature of the Si-Ge bond compared to that of the Si-Si bond. (iv) From Fig. 3 we see that the binding energy of the vacancy to the Ge atom with the vacancy being at the n^{th} coordination site from Ge is 0.24 eV, 0.04 eV, and less than 0.002 eV respectively for $n = 1, 2$ and 3. Therefore, the vacancy is practically bound to Ge only if it is at a nearest neighbor site to Ge. The strength and the range of interaction between a vacancy and Ge is quite weak unlike those between a vacancy and a dopant atom such as arsenic²² or phosphorous⁵³. This difference in the intensity and the extent of the interaction and the difference in the typical concentration of Ge in $\text{Si}_{1-x}\text{Ge}_x$ alloys compared to dopant concentrations suggests that the diffusion of Ge will not be dominated by the pair diffusion mechanism, which is the accepted^{22,30} dominant mechanism of dopant diffusion diffusing by the vacancy mechanism. Rather, the vacancy by randomly moving through the crystal randomly displaces Ge atoms whenever it meets one, thereby causing diffusion. It does not form as strong a pair with the Ge atom as, for example, it does with a phosphorous or an arsenic atom. (v) From the interaction potentials (Fig. 4), we find that the barrier for the Si-V jump (far from a Ge atom) changes by 4eV/unit equi-biaxial strain and the barrier for the Ge-V jump (at very low Ge concentration) changes by 2eV/unit equi-biaxial strain.

The Ge-V interaction potential from Fig. 4 can be used to calculate the correlation factor for Ge diffusion as outlined in Sec. IID. From the transition state theory (TST), the jump rates ν_I , ν_H , ν_F and ν_B mentioned in Sec. IID can be calculated as:

$$\nu_I = \nu_0 \exp[-(E_{xs} - E_1)/k_B T] \quad (15)$$

$$\nu_H = \nu_0 \exp[-(E_{fs} - E_f)/k_B T] \quad (16)$$

$$\nu_F = \nu_0 \exp[-(E_{12} - E_2)/k_B T] \quad (17)$$

$$\nu_B = \nu_0 \exp[-(E_{12} - E_1)/k_B T] \quad (18)$$

where ν_0 denotes the lattice vibrational frequency (which, to a first order approximation we have assumed to be a constant); E_1 , E_2 and E_f respectively denote the energy of the system when the vacancy is at the first nearest neighbor site to the Ge atom, second nearest neighbor site to the Ge atom and far away from the Ge atom; E_{xs} , E_{fs} and E_{12} respectively denote saddle point energies for the vacancy and Ge to exchange positions, for the vacancy and Si to exchange positions far away from a Ge atom, and for the vacancy to move between the first and the second nearest neighboring positions of the Ge atom. Fig. 5 plots the variation of the correlation factor for Ge diffusion as a function of temperature. (As we have noted previously,⁴⁹ the correlation factor approaches the theoretical limit of 0.5 at high temperatures.) In Fig. 6 we show an Arrhenius plot of the same and we extract the activation energy for the strain free, 0.4% biaxial tensile and 0.4% biaxial compressive cases to be 0.168 eV, 0.171 eV, and 0.161 eV respectively. The activation energy associated with the correlation factor for Ge diffusion in

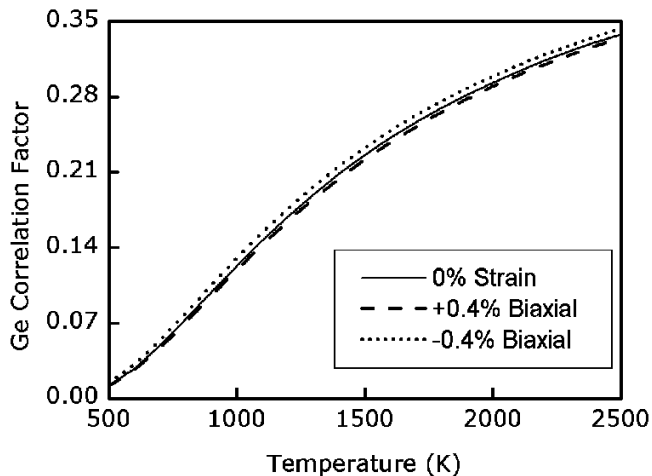


FIG. 5: Theoretical calculation of the correlation factor for the diffusion of Ge in (a) relaxed Si (solid line) (b) 0.4% tensile biaxially strained Si (dashed line) (c) 0.4% compressively biaxially strained Si (dotted line) as a function of temperature. The correlation factors are seen to approach a high temperature limit of 0.5, the theoretical value for a tracer diffusion in a diamond structure.

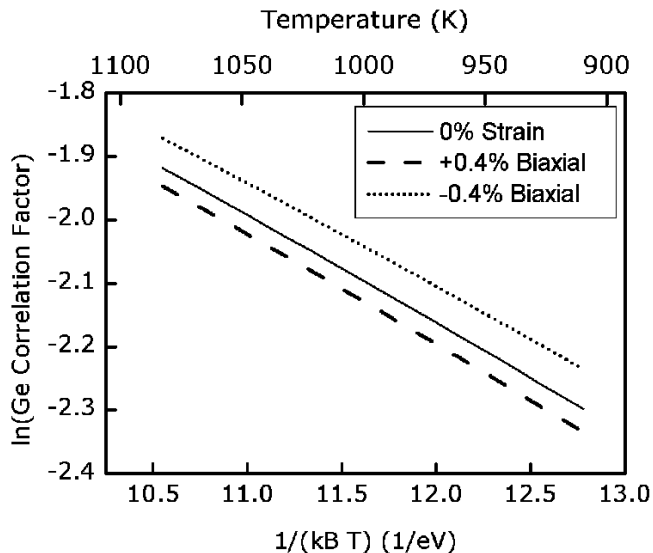


FIG. 6: An Arrhenius type plot of the correlation factor for the diffusion of Ge in (a) relaxed Si (solid line, $E_a^{corr} = 0.168$ eV) (b) 0.4% tensile biaxially strained Si (dashed line, $E_a^{corr} = 0.171$ eV) (c) 0.4% compressively biaxially strained Si (dotted line, $E_a^{corr} = 0.161$ eV) to extract the activation energy corresponding to the correlation factor (E_a^{corr}).

Si at very low Ge concentrations therefore changes by approximately 1 eV/unit strain.

Combining the results of the vacancy formation energy change due to biaxial strain with the migration barrier energy change and the correlation factor activation energy change, we estimate the following values for the effect of equi-biaxial strain on the diffusion-activation energy: 20 eV/unit strain for Si self diffusion in Si, 17 - 20

eV/unit strain for Ge self diffusion in Si. At this point, we would like to quote two experimentally determined values and one empirically fitted value for the change in activation energy for Ge diffusion due to biaxial strain. The experimentally determined values are due to Cowern *et al.*⁵⁴ and Zangenberg *et al.*¹¹ who report a value of 18 eV/unit strain and 160 ± 40 eV/unit strain respectively. Aubertine *et al.*³, who use the strain dependence of the activation energy as a tunable parameter in their empirical model, report that they are best able to reproduce their experimental data if they set this parameter to be 19eV/unit strain.

B. Ge concentration dependence of the vacancy formation energy

The typical concentration of Ge in SiGe films in device structures is 10% - 30%, which is several orders of magnitude larger than the typical dopant concentration (10^{16} - 10^{18} per cm^3). One therefore needs to consider the effect of Ge concentration on the vacancy formation energy (and hence the vacancy concentration) in the system in the manner explained in Sec. II C. From straightforward LDA based calculations, we obtain the following energetics of the SiGe-vacancy system: The energy of the system drops by 0.24, 0.45, 0.6, and 0.83 eV when the vacancy is surrounded respectively by 1, 2, 3 and 4 Ge atoms. Similar figures have been previously reported.^{14,55} The energy of the system drops by 0.04 eV for every second nearest neighbor Ge atom to the vacancy. The energy of the system with Ge in all the second nearest neighbor positions of the vacancy and Si everywhere else is higher than the energy of a system with a vacancy in unary Ge by 0.12 eV. In terms of the notations used in Sec. II C, $F(0) = 0$ eV, $F(1) = 0.24$ eV, $F(2) = 0.45$ eV, $F(3) = 0.6$ eV, $F(4) = 0.83$ eV, $S = 0.04$ eV, and $M = 0.12$ eV. The attractive interaction between the Ge atoms and the vacancy causes the equilibrium vacancy concentration to be larger in regions of high Ge concentration. This lowers the effective vacancy formation energy in $\text{Si}_{1-x}\text{Ge}_x$ compared to a uniform (regionally unbiased) random distribution of vacancies.

Using the theory explained in Sec. II C, we have plotted in Fig. 7 the change in the vacancy formation energy from the vacancy formation energy in Si ($\langle E_f(x, T) \rangle - E_{V_f}^{\text{Si}}$) as a function of Ge concentration calculated at 1000K (solid line). Also plotted in Fig. 7 is the change in the change in the vacancy formation energy vs Ge concentration from a rule-of-mixtures model for the composition dependence of the formation energy (dotted line). The rule-of-mixtures model is consistent with a spatially uniform distribution of vacancies for each $\text{Si}_{1-x}\text{Ge}_x$ composition. The difference between the two curves has a maximum at a particular concentration of Ge, which, of course, is temperature dependent. This is understood by the following reasoning: At very high Ge concentrations, a randomly chosen site would have a high probability

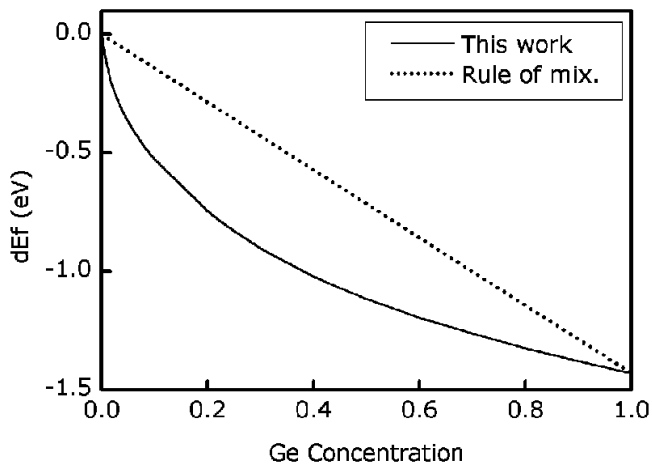


FIG. 7: Solid line shows the change in the vacancy formation energy in $\text{Si}_{1-x}\text{Ge}_x$ from that in pure Si ($dEf = \langle E_f(x, T) \rangle - E_{V_f}^{Si}$) as a function of Ge concentration (x) calculated at 1000K by taking into account the attractive interaction of the vacancy with the Ge atoms. Dotted line shows the same quantity obtained by a simple rule of mixtures.

of having many Ge neighbors. The further reduction in the formation energy because of the vacancies preferentially forming at high Ge concentration sites is therefore marginal. At very low Ge concentrations, the amount of reduction in the formation energy is low because of the small number of Ge atoms present.

C. Vacancy migration energy barrier database

We present, in this subsection, the database of energy barriers for vacancy migration in different environments calculated using the local density approximation. As in the case of calculating the effective vacancy formation energy, we have treated atoms at different distances from the vacancy migration center differently depending on the extent of influence that the atom would exert on the vacancy migration energy barrier. Referring to Fig. 8, the identities of the atoms that are first nearest neighbors to the vacancy (denoted as S1, S2, S3 in the figure), the identity of the migrating atom (denoted as D0), and the identities of the atoms surrounding the migrating atom (denoted as D1, D2, D3) are expected to have the greatest influence on the migration energy barrier. We have assumed that the concentration of vacancies is sufficiently low that none of the seven atoms (S1 - S3, D0 - D3) would be a vacancy. We then get a list of 40 different configurations depending on which of (S1 - S3, D0 - D3) is Si or Ge. We account for the effect of the identities of the atoms beyond these seven nearest neighbors in the following mean field manner: We calculate the migration energy barriers for the 40 different configurations for the following two cases: (i) All the atoms beyond the seven nearest neighbors are Si. (ii) All the atoms beyond the seven nearest neighbors are Ge. Then,

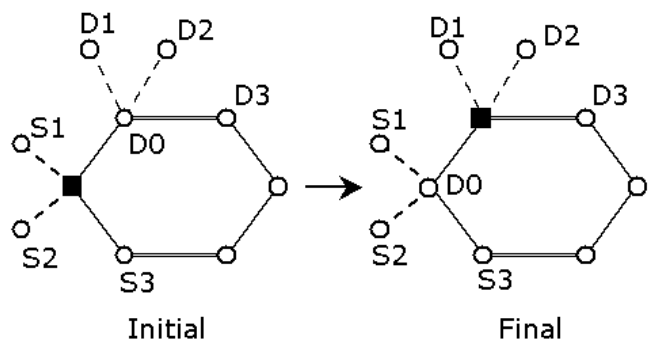


FIG. 8: The energy barrier for the vacancy (filled square) to go from the initial configuration to the final is influenced the most by the identities of the atoms surrounding the vacancy (S1, S2, S3), the identity of the atom with which the vacancy is to exchange position (D0), and the identities of the atoms surrounding D0, namely, D1, D2, and D3. A two dimensional representation of the diamond structure has been adopted for convenience with the different types of lines representing bonds on different planes.

to obtain the energy barrier for any one of these 40 configurations in a $\text{Si}_{1-x}\text{Ge}_x$ alloy (with a Ge concentration of x), we linearly interpolate the migration energy barrier of that particular configuration from cases (i) and (ii) mentioned above.

This approach seems to be reasonably satisfactory for at least one of the configurations (all (S1 - S3, D0 - D3) are Ge atoms) that we have tested (Fig. 9). The top configuration shown in Fig. 9 corresponds to the case where the seven nearest neighbors within the dotted circle (S1 - S3, D0 - D3) are all Ge atoms and all atoms beyond the nearest neighbor sites are Si (case (i) above). The migration energy barrier is 0.03 eV. The bottom configuration corresponds to the same nearest neighbor configuration but all atoms beyond the nearest neighbor sites being Ge (case (ii) above). The migration energy barrier is 0.13 eV. The middle configuration is an explicit calculation of the energy barrier with the same nearest neighbor configuration (i.e., all (S1 - S3, D0 - D3) are Ge atoms) but all the atoms beyond the nearest neighbor sites are either Si or Ge with a probability of 0.5. This is consistent with what would occur in a $\text{Si}_{1-x}\text{Ge}_x$ alloy with $x = 0.5$. Unlike in the top and the bottom configurations, the barrier for the forward migration (0.11 eV) is different from that for the reverse migration (0.07 eV) because unlike in the top and the bottom configurations, the identities of the second nearest neighbor sites are not identical for the forward and the reverse migrations. The mean of the forward and the reverse barriers (0.09 eV), however, is closer to the linear interpolation of the barriers from the top and the bottom configurations (0.08 eV) than it is to either of the them. We should mention that the $\text{Si}_{0.5}\text{Ge}_{0.5}$ case is one which is farthest away from the reference cases (cases (i) and (ii)) and so is a stringent test, in a certain sense, of the approximation used. So a reasonable agreement in this case definitely indicates

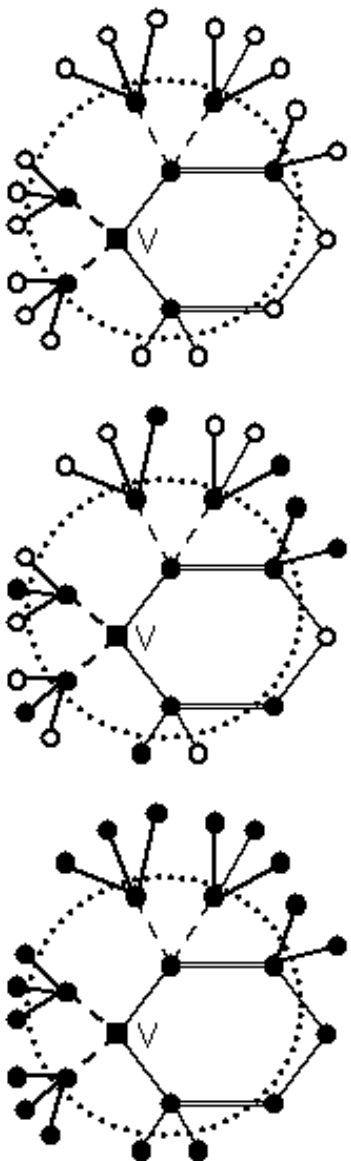


FIG. 9: Although all the three configurations shown above have the same nearest neighbor atoms to the vacancy migration center (atoms within the dotted circle), they have different vacancy migration energy barriers. The top configuration has Si atoms (open circles) everywhere outside the dotted circle and has a vacancy migration energy barrier of 0.03 eV. The bottom configuration has Ge atoms (filled circles) everywhere outside the dotted circle and has a vacancy migration energy barrier of 0.13 eV. The middle configuration has 50% of the atoms outside the dotted circle as Si. The barrier for the forward migration is 0.11 eV and that for the reverse migration is 0.07 eV. The mean (0.09 eV) is closer to the linear interpolation of the barriers from the top and the bottom configurations (0.08 eV) than it is to either of them. (Si: open circles; Ge: filled circles; vacancy: filled square with a label “V”.)

that the approximation used is reasonable.

We have calculated the saddle point energies for each of these 80 different configurations very accurately using the nudged elastic band (NEB) method.³⁷ We also note that we have eliminated strain effects by suitably adjusting the lattice parameter for the number of Si and Ge atoms for each of the 80 configurations. Table I summarizes the vacancy migration energy barriers. The barriers are negligibly small for some of the configurations where there is a significant asymmetry between the initial and the final environments of the vacancy (in terms of the number of Ge atoms) especially for the case of 0% Ge. By plotting the atomic positions, we have found out that the reason for this behavior is the following: When there is a significant asymmetry, the initial (or the final) structure “collapses” to the other or to some configuration intermediate between the two and there is no barrier to get from the one to the other. We feel that it happens more in the case of 0% Ge because the lower lattice constant of Si compared to Ge facilitates this collapsing more easily than in the case of 100% Ge.

D. Kinetic Monte Carlo simulation

In this section we present the results of the kinetic Monte Carlo simulations done using the vacancy migration energy barrier database presented in Sec. III C.

1. Diffusivity, AMF energy

From the KMC simulations, we were able to compute the diffusivity of Si and Ge in $\text{Si}_{1-x}\text{Ge}_x$ as a function of Ge concentration (x) and the temperature. (The diffusivity is given by $D = \langle X^2 \rangle / 6\tau$, see Sec. II E). We note that these simulations have a constant vacancy concentration (of 10^{-6} /atom); in other words, the change in the vacancy concentration due to the change in the Ge concentration as explained in Sec. III B has not been factored in. The lattice vibrational frequency ν_0 was estimated from first principles based on a harmonic approximation to be $7.325 \times 10^{11} \text{ sec}^{-1}$. Figures 10 and 11 show the plots of the Ge and the Si diffusivities respectively. As expected, the diffusivity increases with temperature. From an Arrhenius type plot of the diffusivities, we have extracted the activation minus formation (AMF) energy. These have been plotted in Fig. 12. We make the following observations with reference to Figs. 10 - 12. (i) The AMF energy for the diffusion of Si in Si (0.11 eV) matches closely with the migration energy for a vacancy in pure Si. (Compare with the entry in Table I corresponding to all (S1 - S3, D0 - D3) being Si under 0% Ge.) A similar close match is also obtained for the AMF energy for the diffusion of Ge in Ge (0.13 eV). (Compare with the entry in table 1 corresponding to all (S1 - S3, D0 - D3) being Ge under 100% Ge.) Along with providing a verification of our computer simulation programs,

TABLE I: Vacancy migration energy barrier database. S1, S2, and S3 are the identities of the atoms surrounding the vacancy, D0 is the identity of the atom with which the vacancy is to exchange positions, and D1, D2, and D3 are the identities of the atoms surrounding D0. Under 0% Ge are listed the energy barriers corresponding to the case where all atoms other than S1 - S3, D0 - D3 are Si and under 100% Ge are listed the barriers when those atoms are all Ge instead.

| S1 | S2 | S3 | D0 | D1 | D2 | D3 | 0% Ge (eV) | 100% Ge (eV) |
|----|----|----|----|----|----|----|------------|--------------|
| Si | Si | Si | Si | Si | Si | Si | 0.11 | 0.26 |
| Si | Si | Si | Ge | Si | Si | Si | 0.08 | 0.22 |
| Si | Si | Si | Si | Si | Si | Ge | 0.03 | 0.87 |
| Si | Si | Si | Ge | Si | Si | Ge | 0.00 | 0.10 |
| Si | Si | Si | Si | Ge | Ge | Si | 0.00 | 0.05 |
| Si | Si | Si | Ge | Ge | Ge | Si | 0.00 | 0.03 |
| Si | Si | Si | Si | Ge | Ge | Ge | 0.00 | 0.00 |
| Si | Si | Si | Ge | Ge | Ge | Ge | 0.00 | 0.00 |
| Si | Si | Ge | Si | Si | Si | Si | 0.23 | 1.03 |
| Si | Si | Ge | Ge | Si | Si | Si | 0.18 | 0.81 |
| Si | Si | Ge | Si | Si | Si | Ge | 0.09 | 0.86 |
| Si | Si | Ge | Si | Ge | Si | Si | 0.10 | 0.89 |
| Si | Si | Ge | Ge | Si | Si | Ge | 0.06 | 0.18 |
| Si | Si | Ge | Ge | Ge | Si | Si | 0.06 | 0.67 |
| Si | Si | Ge | Si | Ge | Ge | Si | 0.01 | 0.74 |
| Si | Si | Ge | Si | Si | Ge | Ge | 0.00 | 0.70 |
| Si | Si | Ge | Ge | Ge | Ge | Si | 0.00 | 0.09 |
| Si | Si | Ge | Ge | Si | Ge | Ge | 0.00 | 0.07 |
| Si | Si | Ge | Si | Ge | Ge | Ge | 0.00 | 0.64 |
| Si | Si | Ge | Ge | Ge | Ge | Ge | 0.00 | 0.01 |
| Si | Ge | Ge | Si | Si | Si | Si | 0.00 | 0.51 |
| Si | Ge | Ge | Ge | Si | Si | Si | 0.00 | 0.44 |
| Ge | Ge | Si | Si | Si | Si | Ge | 0.21 | 0.34 |
| Ge | Ge | Si | Si | Ge | Si | Si | 0.00 | 0.32 |
| Ge | Ge | Si | Ge | Si | Si | Ge | 0.16 | 0.29 |
| Ge | Ge | Si | Ge | Ge | Si | Si | 0.00 | 0.27 |
| Ge | Ge | Si | Si | Ge | Ge | Si | 0.07 | 0.18 |
| Ge | Ge | Si | Si | Si | Ge | Ge | 0.08 | 0.20 |
| Ge | Ge | Si | Ge | Ge | Ge | Si | 0.04 | 0.15 |
| Ge | Ge | Si | Ge | Si | Ge | Ge | 0.05 | 0.16 |
| Si | Ge | Ge | Si | Ge | Ge | Ge | 0.00 | 0.08 |
| Si | Ge | Ge | Ge | Ge | Ge | Ge | 0.00 | 0.05 |
| Ge | Ge | Ge | Si | Si | Si | Si | 0.00 | 0.69 |
| Ge | Ge | Ge | Ge | Si | Si | Si | 0.00 | 0.00 |
| Ge | Ge | Ge | Si | Si | Si | Ge | 0.00 | 0.48 |
| Ge | Ge | Ge | Ge | Si | Si | Ge | 0.00 | 0.41 |
| Ge | Ge | Ge | Si | Si | Ge | Ge | 0.00 | 0.30 |
| Ge | Ge | Ge | Ge | Si | Ge | Ge | 0.00 | 0.25 |
| Ge | Ge | Ge | Si | Ge | Ge | Ge | 0.05 | 0.16 |
| Ge | Ge | Ge | Ge | Ge | Ge | Ge | 0.03 | 0.13 |

it also corroborates our concept of the AMF energy as explained in Sec. I. (ii) We have not been able to obtain satisfactory numerical agreement of the AMF energy for the diffusion of Si in Ge (0.34 eV) or for that of diffusion of Ge in Si (0.05 eV) based on the models presented in Refs. 21,22,23. We however have the following plausible qualitative explanation: The *attractive* interaction between vacancies and Ge atoms (see Fig. 3) causes a vacancy to be *more available* near the vicinity of a Ge atom to facilitate its diffusion. This probably results in *lower-*

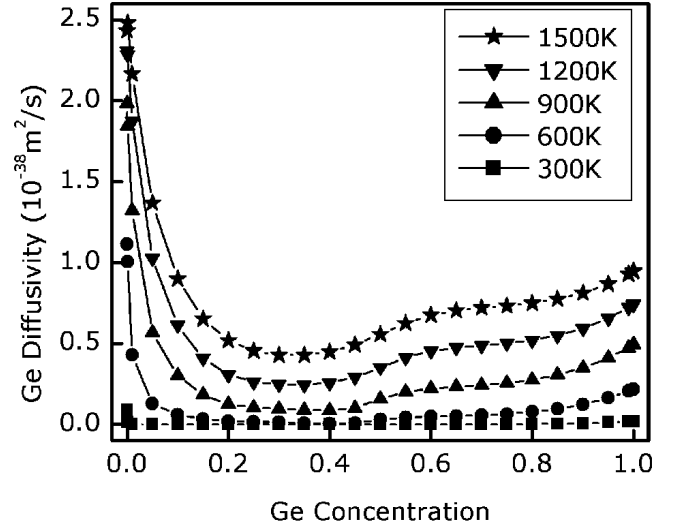


FIG. 10: Diffusivity of Ge in $\text{Si}_{1-x}\text{Ge}_x$ calculated from the results of the KMC simulation as a function of Ge concentration (x) at five different temperatures: 300K - square; 600K - circle; 900K - upward triangle; 1200K - downward triangle; 1500K - pentagram. (Lines are drawn as a guide to the eye.)

ing the AMF energy for the Ge diffusion in Si compared to the migration barrier for a Ge-vacancy exchange process in Si (0.08 eV (see the second entry under 0% Ge in Table I)). Conversely, the *repulsive* interaction between a Si and a vacancy (see Fig. 13) makes a vacancy *less available* near the vicinity of a Si atom. This probably results in *increasing* the AMF energy for the Si diffusion in Ge compared to the migration barrier for a Si-vacancy exchange process in Ge (0.16 eV (see the penultimate entry under 100% Ge in Table I)). (iii) While we do not have a microscopic explanation for the abrupt drop in the diffusivity of both Si and Ge near low Ge concentrations, we do find them to be consistent with the rise in AMF energy of both Si and Ge near low Ge concentrations. (iv) The reason for the non smooth behavior of the AMF energies near 50% Ge concentration is probably because of those concentrations being farthest away from the reference configurations (0% and 100% Ge) that were used to build the migration energy barrier database.

In Fig. 14, we plot the change in the activation energy for Ge diffusion in $\text{Si}_{1-x}\text{Ge}_x$ compared to that in Si as a function of Ge concentration. The activation energy is calculated as a sum of the vacancy formation energy from Fig. 7 and the Ge AMF energy from Fig. 12. Also plotted on the same axes are the experimentally observed changes in the activation energy for Ge diffusion from Refs. 11,12,13. The purpose of this plot is not actually to compare our results with the experiments, which, as we have already mentioned in Sec. I is premature at this stage. But this plot clearly brings out the need to consider the other mechanisms before a fair comparison with experiments is possible.

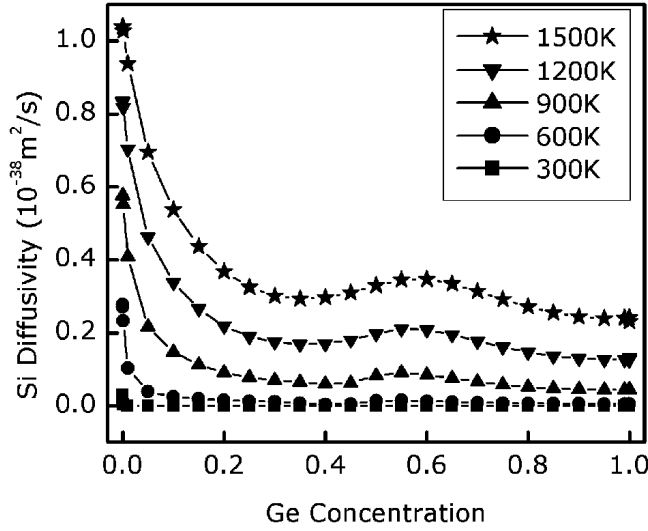


FIG. 11: Diffusivity of Si in $\text{Si}_{1-x}\text{Ge}_x$ calculated from the results of the KMC simulation as a function of Ge concentration (x) at five different temperatures: 300K - square; 600K - circle; 900K - upward triangle; 1200K - downward triangle; 1500K - pentagram. (Lines are drawn as a guide to the eye.)

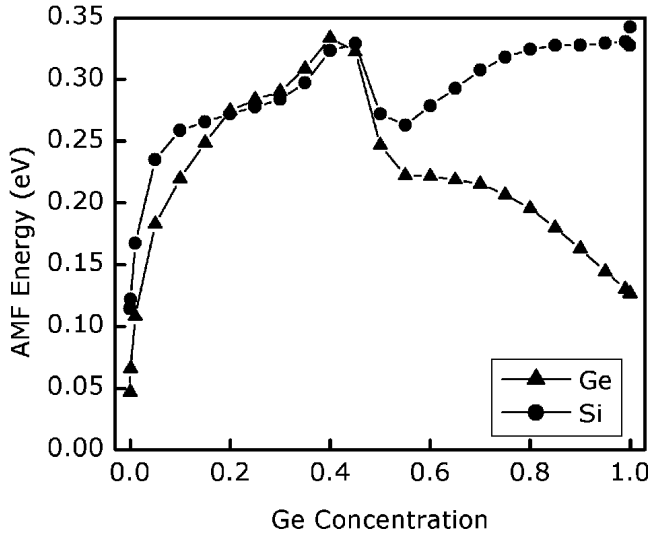


FIG. 12: Variation of the activation-minus-formation (AMF) energy (eV) for the diffusion of Ge (upward triangle) and Si (circle) in $\text{Si}_{1-x}\text{Ge}_x$ as a function of Ge concentration (x) obtained from the results of the KMC simulation. (Lines are drawn as a guide to the eye.)

2. Correlation factor

The correlation factor for Ge and Si calculated by the procedures outlined in Secs. IID and IIE are plotted respectively in Figs. 15 and 16 as a function of the Ge concentration for five different temperatures. We make the following observations with reference to these plots. (i) The correlation factors that we have calculated for the unary substances (i.e., Si correlation factor in 0%

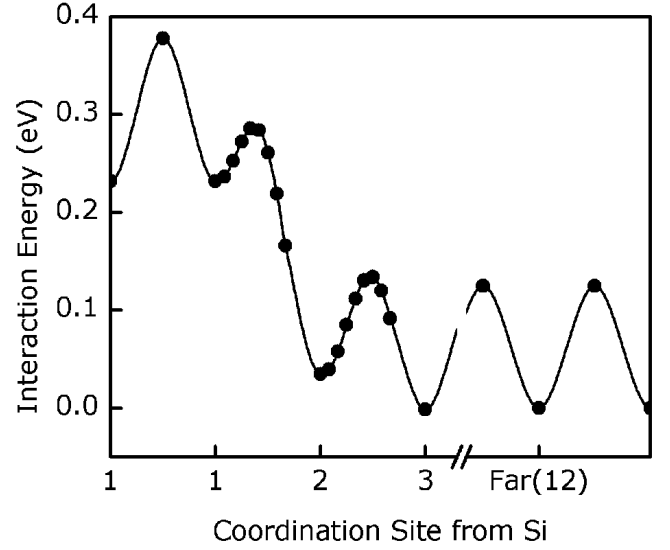


FIG. 13: Interaction potential energy (in eV) between a substitutional Si atom and a vacancy as a function of vacancy position in relaxed Ge from LDA calculations. (Lines are drawn as a guide to the eye.)

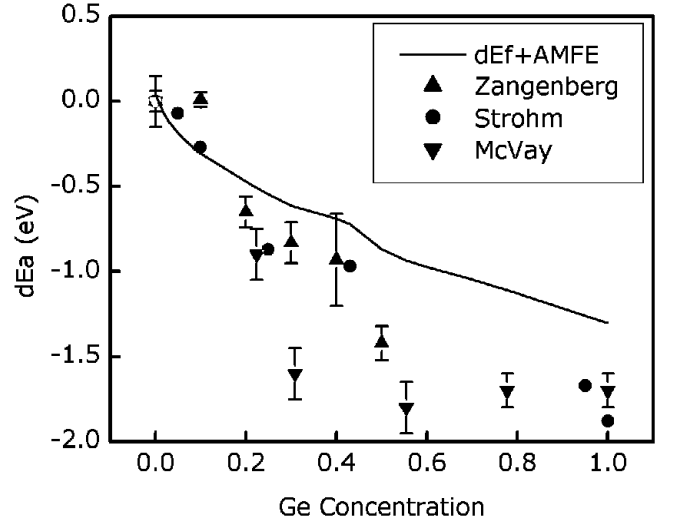


FIG. 14: Solid line shows the change in the activation energy for the diffusion of Ge in $\text{Si}_{1-x}\text{Ge}_x$ by a vacancy mechanism from that in pure Si as a function of Ge concentration (x) calculated at 1000K as the sum of the change in the vacancy formation energy and the Ge activation-minus-formation (AMF) energy. Also shown are the experimental results for the same quantity from Zangenberg *et al.*¹¹ (upward triangle), Strohm *et al.*¹² (circle), and McVay and DuCharme¹³ (downward triangle).

Ge concentration and Ge correlation factor in 100% Ge concentration) equal 0.5. This is the theoretical value for the correlation factor for a tracer diffusion in the diamond structure.⁴⁸ (This provides an additional verification of our calculations.) That the correlation factor for a tracer (diffusing by the vacancy mechanism) should

be less than unity is clear from the observation that the tracer atom has a higher probability of jumping back to the vacancy site thereby nullifying a forward jump. The mean squared displacement (and hence the diffusivity) of this correlated motion would therefore be less than that of a random jump, giving a correlation factor less than unity. The specific value of 0.5 is a result of the tetrahedral geometry of the silicon crystal structure. (ii) At higher temperatures, the Boltzmann factor evens out the different energy barriers, making the system resemble a unary substance. One would therefore expect the correlation factor to approach the value for a unary substance in the diamond structure, namely 0.5. We observe this in our plots. (iii) At low Ge concentrations, the correlation factor for Ge drops below 0.5. The reason for this is understood by the following argument: The attractive interaction between Ge and a vacancy and the lower energy barrier for a vacancy to exchange positions with Ge than to jump to the second nearest neighbor site of Ge from the first (which results in breaking the Ge-vacancy bond, see Fig. 3), tend to cause the Ge and the vacancy to jump back and forth several times before breaking away from each other. But, in the diamond structure, because there is no atomic location that is a simultaneous neighbor to both the vacancy and the Ge atom (when they are first nearest neighbors to each other), breakage of the Ge-vacancy pair is essential for the Ge atom to be effectively displaced from its current location. This back and forth motion does not contribute to the mean squared displacement of the Ge atoms and consequently the Ge correlation factor drops. (iv) At low Ge concentrations, the correlation factor for Si drops below 0.5. We offer the following explanation for this behavior: The attractive interaction between the Ge and the vacancy causes the vacancies to be predominantly found near Ge atoms. So, only the Si atoms found near those Ge atoms are affected by the vacancy motion. These Si atoms, owing to the lower energy barrier for the vacancy to jump to the first nearest neighbor site of the Ge atom from the second than to jump to the third from the second (see Fig. 3), just keep jumping back and forth between the first and the second nearest neighbor sites of the Ge (depending on whether the vacancy is correspondingly at the second or the first nearest neighbor sites). This back and forth motion does not effectively displace the Si atoms and so does not contribute to the mean squared displacement. This causes the Si correlation factor to drop. (v) The correlation factors of both Si and Ge increase with increasing Ge concentration. We explain this in the following manner: As the concentration of Ge increases, the vacancy is attracted by the other Ge atoms too and therefore it is less likely to be bound to a single Ge atom. This reduces the redundant back and forth motion of the Ge atoms, thus increasing the mean squared displacement and consequently the Ge correlation factor. (This effect is similar, in some ways, to the percolation mechanism for diffusion.²⁹) The vacancy, in the process of moving from one Ge atom to the other, ends up displacing Si

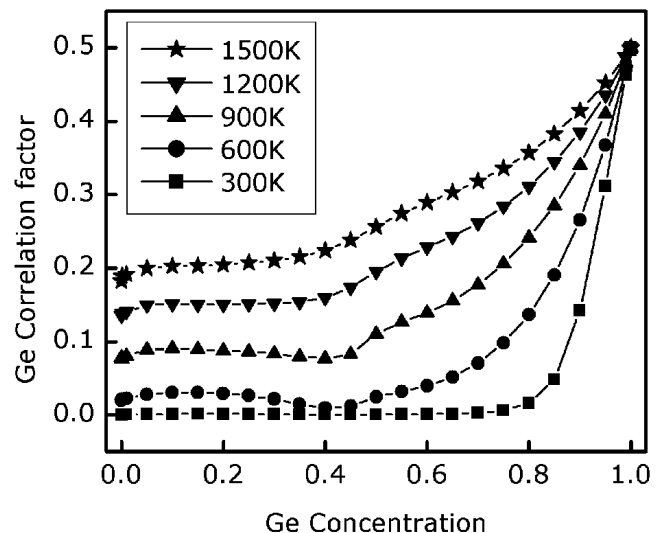


FIG. 15: Correlation factor for the diffusion of Ge in $\text{Si}_{1-x}\text{Ge}_x$ calculated from the results of the KMC simulation as a function of Ge concentration (x) at five different temperatures: 300K - square; 600K - circle; 900K - upward triangle; 1200K - downward triangle; 1500K - pentagram. (Lines are drawn as a guide to the eye.)

atoms thus increasing their mean squared displacement and consequently the Si correlation factor. (vi) The correlation factor for Si in $\text{Si}_{1-x}\text{Ge}_x$ alloys with high Ge concentration is greater than 0.5 and approaches unity. This interesting behavior is explained by the following reasoning: At very high Ge concentration (i.e., very low Si concentration), the faster jumping rate of the vacancy with the Ge atoms compared to that with the Si atoms (because of the lower barrier height (compare last two entries under 100% Ge in Table I)) causes the vacancy to perform a lot of jumps with Ge atoms between successive jumps with a Si atom. This results in the vacancy approaching Si via an essentially random path, making the Si jumps closer to a random walk process. This causes the correlation factor to approach unity. In Fig. 13, we show the interaction energy between a Si and a vacancy in a Ge environment. In Fig. 17 we show the variation of the Si correlation factor with temperature calculated as outlined in Sec. IID. We do see that the correlation factor tends to unity in the lower temperature limit.

IV. SUMMARY

Our purpose of the present work was to understand, from first principles, the effect of biaxial strain and composition on the self-diffusivity of Si and Ge in $\text{Si}_{1-x}\text{Ge}_x$ alloys. In order to attack the problem, we broke it down into one of studying the effect of these factors on the main components that define the diffusivity: the vacancy formation energy, and the activation minus formation (AMF) energy. (The necessity and the definition of

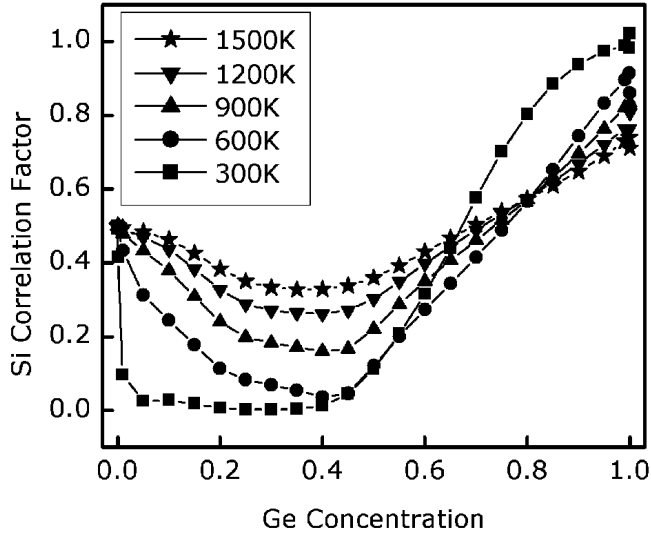


FIG. 16: Correlation factor for the diffusion of Si in $\text{Si}_{1-x}\text{Ge}_x$ calculated from the results of the KMC simulation as a function of Ge concentration (x) at five different temperatures: 300K - square; 600K - circle; 900K - upward triangle; 1200K - downward triangle; 1500K - pentagram. (Lines are drawn as a guide to the eye.)

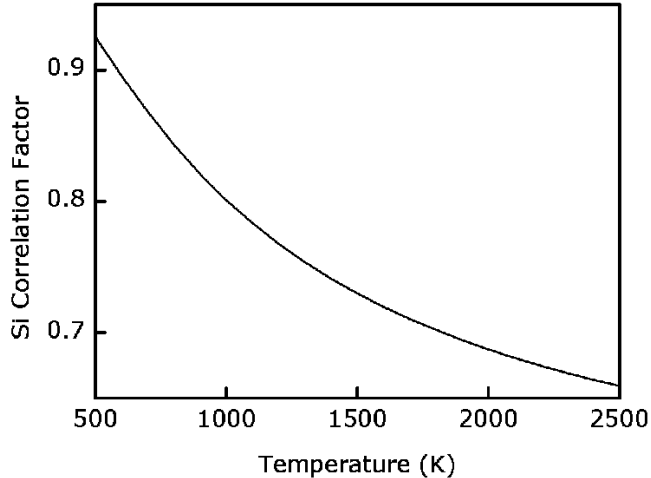


FIG. 17: Theoretical calculation of the correlation factor for the diffusion of Si in relaxed Ge.

AMF energy were presented.) We attacked the problem by the following three main steps: (i) We performed density functional theory (DFT) calculations within the local density approximation (LDA) to obtain the required energetics of the various configurations. (ii) We worked out

the details necessary to calculate the correlation factor and the change in the vacancy formation energy with composition. (iii) We performed kinetic Monte Carlo (KMC) simulations using our total energy calculations. By this approach, we were able to estimate the following values for the effect of biaxial strain on the activation energy (the sum of the vacancy formation energy and AMF energy): 20 eV/unit strain for Si self diffusion in Si and 17 - 20 eV/unit strain for Ge self-diffusion in Si. We calculated the change in the vacancy formation energy in $\text{Si}_{1-x}\text{Ge}_x$ as a function of composition. From the KMC simulations, we were able to extract the variation of the AMF energy for Si and Ge self-diffusion in $\text{Si}_{1-x}\text{Ge}_x$ as a function of composition. We combined the Ge AMF energy with the vacancy formation energy to find the variation of the activation energy for Ge diffusion in $\text{Si}_{1-x}\text{Ge}_x$ as a function of composition. Lastly, we presented the variation of the correlation factor for Si and Ge diffusion in $\text{Si}_{1-x}\text{Ge}_x$ as a function of composition and temperature and made several interesting observations that are quite general for a vacancy mediated diffusion in a random binary alloy arranged in a diamond structure.

There are many outstanding issues of the complete model that need to be resolved even for the vacancy mechanism alone. We conclude this article by recognizing the following limitations of the present work: (i) As we mentioned in the introduction, the inability of the LDA to reproduce experimentally observed values of the activation energy in Si precludes our results from being directly compared with experiments. (ii) We have not addressed the effect of strain and composition on the pre-exponential factor and have not considered entropic effects.

Acknowledgments

P.R. gratefully acknowledges the feedback from Prof. P. C. McIntyre and Dr. P. B. Griffin and thanks them for carefully reviewing the manuscript. P.R. also thanks Dr. R. Sabiryanov, S. Park, G. Lakatos, and D. Aubertine for useful discussions. The computations were performed on the Cray T3E, IBM p690 and on *Multipod*, a PC cluster of MSL, Stanford. Utilization of the Cray and the IBM machines were possible through a grant from NPACI. Efforts of G. Jun in maintaining *Multipod* are sincerely appreciated. This work was funded by the Department of Energy, Basic Energy Sciences grant DE-FG03-99ER45788.

* panchram@stanford.edu

¹ URL <http://www-3.ibm.com/chips/bluelogic/showcase/sige/>.

² B. S. Meyerson, Proc. IEEE **80**, 1592 (1992).

³ D. B. Aubertine, M. A. Mander, N. Ozguven, A. Marshall, P. C. McIntyre, J. O. Chu, and P. M. Mooney, J. Appl. Phys. (accepted).

⁴ J. M. Baribeau, J. Appl. Phys. **74**, 3805 (1993).

- ⁵ S. S. Iyer and F. K. Legoues, *J. Appl. Phys.* **65**, 4693 (1989).
- ⁶ S. M. Prokes, *Mater. Sci. Technol.* **11**, 389 (1995).
- ⁷ S. J. Chang, K. L. Wang, R. C. Bowman, Jr., and P. M. Adams, *Appl. Phys. Lett.* **54**, 1253 (1989).
- ⁸ R. Schorer, E. Friess, K. Eberl, and G. Abstreiter, *Phys. Rev. B* **44**, 1772 (1991).
- ⁹ Y. S. Lim, J. Y. Lee, H. S. Kim, and D. W. Moon, *Appl. Phys. Lett.* **77**, 4157 (2000).
- ¹⁰ Y. S. Lim, J. Y. Lee, H. S. Kim, and D. W. Moon, *Appl. Phys. Lett.* **80**, 2481 (2002).
- ¹¹ N. R. Zangenberg, J. L. Hansen, J. Fage-Pedersen, and A. N. Larsen, *Phys. Rev. Lett.* **87**, 125901 (2001).
- ¹² A. Strohm, T. Voss, W. Frank, J. Räisänen, and M. Dietrich, *Physica B* **308-310**, 542 (2001).
- ¹³ G. L. McVay and A. R. DuCharme, *Phys. Rev. B* **9**, 627 (1974).
- ¹⁴ P. Venezuela, G. M. Dalpian, A. J. R. da Silva, and A. Fazzio, *Phys. Rev. B* **65**, 193306 (2002).
- ¹⁵ P. M. Fahey, P. B. Griffin, and J. D. Plummer, *Rev. Mod. Phys.* **61**, 289 (1989).
- ¹⁶ S. Goedecker, T. Deutsch, and L. Billard, *Phys. Rev. Lett.* **88**, 235501 (2002).
- ¹⁷ P. Fahey, S. S. Iyer, and G. J. Scilla, *Appl. Phys. Lett.* **54**, 843 (1989).
- ¹⁸ M. M. D. Souza and E. M. S. Narayanan, *Defect and Diffusion Forum* **153-155**, 69 (1998).
- ¹⁹ W. K. Leung, R. J. Needs, G. Rajagopal, S. Itoh, and S. Ihara, *Phys. Rev. Lett.* **83**, 2351 (1999).
- ²⁰ W. M. C. Foulkes, L. Mitas, R. J. Needs, and G. Rajagopal, *Rev. Mod. Phys.* **73**, 33 (2001).
- ²¹ S. T. Dunham and C. D. Wu, *J. Appl. Phys.* **78**, 2362 (1995).
- ²² O. Pankratov, H. Huang, T. D. de la Rubia, and C. Mailhot, *Phys. Rev. B* **56**, 13172 (1997).
- ²³ O. Sugino and A. Oshiyama, *Phys. Rev. B* **46**, 12335 (1992).
- ²⁴ A. Antonelli and J. Bernholc, *Mat. Res. Soc. Symp. Proc.* **163**, 523 (1990).
- ²⁵ A. Antonelli, E. Kaxiras, and D. J. Chadi, *Phys. Rev. Lett.* **81**, 2088 (1998).
- ²⁶ W. Windl, M. M. Bunea, R. Stumpf, S. T. Dunham, and M. P. Masquelier, *Phys. Rev. Lett.* **83**, 4345 (1999).
- ²⁷ M. S. Daw, W. Windl, N. N. Carlson, M. Laudon, and M. P. Masquelier, *Phys. Rev. B* **64**, 045205 (2001).
- ²⁸ P. H. Dederichs and K. Schroeder, *Phys. Rev. B* **17**, 2524 (1978).
- ²⁹ D. Mathiot and J. C. Pfister, *J. Phys. Lett.* **43**, L453 (1982).
- ³⁰ M. Yoshida, *Jpn. J. Appl. Phys.* **10**, 702 (1971).
- ³¹ M. M. Bunea and S. T. Dunham, *Phys. Rev. B* **61**, R2397 (2000).
- ³² G. Kresse and J. Hafner, *Phys. Rev. B* **47**, 558 (1993).
- ³³ G. Kresse and J. Hafner, *Phys. Rev. B* **49**, 14251 (1994).
- ³⁴ G. Kresse and J. Furthmüller, *Comput. Mater. Sci.* **6**, 15 (1996).
- ³⁵ G. Kresse and J. Furthmüller, *Phys. Rev. B* **54**, 11169 (1996).
- ³⁶ H. Monkhorst and J. Pack, *Phys. Rev. B* **13**, 5188 (1976).
- ³⁷ H. Jónsson, G. Mills, and K. W. Jacobsen, in *Classical and Quantum Dynamics in Condensed Phase Simulations*, edited by B. J. B. et al. (World Scientific, Singapore, 1998), chap. 16.
- ³⁸ The Murnaghan's equation of state³⁹ is a relation between the energy E and the volume V of the supercell and has the following form: $E = E_0 + [(V - V_0)/b] - \{[(V^{1-a} - V_0^{1-a})V_0^a]/[(1-a)b]\}$. E_0 , V_0 , a , and b are fitting parameters.
- ³⁹ F. D. Murnaghan, *Proc. Natl. Acad. Sci.* **30**, 244 (1944).
- ⁴⁰ M. J. Puska, S. Pöykkö, M. Pesola, and R. M. Nieminen, *Phys. Rev. B* **58**, 1318 (1998).
- ⁴¹ J. L. Mercer, J. S. Nelson, A. F. Wright, and E. B. Stechel, *Modelling Simul. Mater. Sci. Eng.* **6**, 1 (1998).
- ⁴² J. Dabrowski, *Solid State Phenomena* **71**, 23 (2000).
- ⁴³ A. J. R. d. S. A. Fazzio, A. Janotti and R. Mota, *Phys. Rev. B* **61**, R2401 (2000).
- ⁴⁴ S. de Gironcoli, P. Giannozzi, and S. Baroni, *Phys. Rev. Lett.* **66**, 2116 (1991).
- ⁴⁵ Our calculations show that the energies of the systems with 62 Si atoms and 2 Ge atoms with the Ge atoms being at different positions relative to each other differ by less than 0.009 eV confirming that $\text{Si}_{1-x}\text{Ge}_x$ does indeed form a model random alloy.
- ⁴⁶ A. B. Bortz, M. H. Kalos, and J. L. Lebowitz, *J. Comput. Phys.* **17**, 10 (1975).
- ⁴⁷ A. F. Voter, *Phys. Rev. B* **34**, 6819 (1986).
- ⁴⁸ J. R. Manning, *Diffusion Kinetics for Atoms in Crystals* (D. Van Nostrand, Princeton, New Jersey, 1968).
- ⁴⁹ We justify our choice of limiting the number of vacancy hops to five based on the following observation: The calculated correlation factors at a temperature of 2×10^5 K considering upto one, three, and five vacancy jump sequences respectively are 0.579, 0.518, and 0.509. At such a high temperature as 2×10^5 K, one would expect to get the theoretical correlation factor for a tracer diffusion in a diamond lattice which has a value⁴⁸ of 0.5. Using five hops, we are able to get reasonably close to the theoretical value.
- ⁵⁰ M. J. Aziz, *Appl. Phys. Lett.* **70**, 2810 (1997).
- ⁵¹ A. Y. Kuznetsov, J. Cardenas, D. C. Schmidt, B. G. Svensson, J. L. Hansen, and A. N. Larsen, *Phys. Rev. B* **59**, 7274 (1999).
- ⁵² C. G. V. de Walle and R. M. Martin, *Phys. Rev. B* **34**, 5621 (1986).
- ⁵³ J. S. Nelson, P. A. Schultz, and A. F. Wright, *Appl. Phys. Lett.* **73**, 247 (1998).
- ⁵⁴ N. E. B. Cower, W. J. Kersten, R. C. M. de Kruijff, J. G. M. van Berkum, W. B. de Boer, D. J. Gravesteijn, and C. W. T. Bulle-Liewma, *Electrochem. Soc. Proc.* **96-4**, 195 (1996).
- ⁵⁵ P. Boguslawski and J. Bernholc, *Phys. Rev. B* **59**, 1567 (1999).